

Figure 3 | Dual functional imaging with two FRET pairs. **(a)** Pseudocolored ratio images of representative HeLa cells expressing SC-SCAT3 (top) and SapRC2 (bottom), at the indicated times (in minutes) after treatment with TNF- α . The color bars represent the cyan-to-ultramarine fluorescence intensity ratio (mseCFP/Sirius; top) or red-to-green intensity ratio (DsRed/Sapphire; bottom). Scale bar, 10 μ m. **(b)** Time course of the fluorescence intensity after four-color spectral linear unmixing in the region circled in **(a)** (a.u., arbitrary units). **(c)** Fluorescence intensity ratio of mseCFP/Sirius and DsRed/Sapphire after four-color spectral unmixing in the region circled in **(a)**.

cells. Although the excitation of Sirius at 780 nm was not effective when compared with that of EBFP2 (**Fig. 2b**), it was sufficient to identify Sirius-expressing specimens. Using EGFP-expressing bacteria, the fluorescence signal disappeared before the bacteria were completely digested in phagosomes (**Fig. 2c** and **Supplementary Video 1** online). In contrast, using Sirius-expressing bacteria, we could visualize the entire process of phagocytosis (**Fig. 2c** and **Supplementary Video 1**).

Sirius is potentially an ideal donor to pair with mseCFP for fluorescence resonance energy transfer (FRET), since the emission spectrum of Sirius overlaps substantially with the absorption spectrum of mseCFP (**Supplementary Fig. 7a** online). However, the spectral overlap ($J = 0.71 \times 10^{-13} \text{ M}^{-1} \text{ cm}^3$) is smaller than in some other FRET pairs, such as CFP-YFP ($J = 1.89 \times 10^{-13} \text{ M}^{-1} \text{ cm}^3$), owing to the fourth power wavelength dependency of J . Also, when assuming $\kappa^2 = 2/3$, the Förster distance (R_0) of Sirius-mseCFP pair ($R_0 = 3.7 \text{ nm}$) is smaller than that of CFP-YFP ($R_0 = 4.7 \text{ nm}$) (**Supplementary Table 1** online) because of the lower Φ_{F1} of Sirius. Despite these drawbacks, the Sirius-mseCFP fusion protein (joined by a Leu-Glu peptide linker) showed a moderate sensitized emission from mseCFP, with 43% FRET efficiency (**Supplementary Fig. 7b,c** and **Supplementary Note 1** online). Encouraged by this result, we constructed an indicator for caspase-3 activation⁵ by fusing the caspase-3 substrate Asp-Glu-Val-Asp between Sirius and mseCFP, yielding SC-SCAT3. We then monitored the change in FRET signal of SC-SCAT3 in apoptotic HeLa cells. As shown previously⁶, we visualized caspase-3 activation first in the cytoplasm and then in the nucleus, which was followed by cell shrinking.

Recently, multiple-FRET imaging by using two independently excitable FRET pairs has been reported⁷. Because the FRET donors have distinct excitation profiles, there was only slight

cross-excitation, allowing an accurate ratio-metric measurement of the two FRET indicators. We expanded the dual FRET imaging arsenal with a different strategy that makes use of two FRET pairs, Sirius-mseCFP and Sapphire-DsRed (**Supplementary Fig. 7d**), both of which can be excited with a single wavelength (380 nm; or 720 nm by two-photon excitation) (**Supplementary Fig. 7e**). In combination with linear spectral unmixing⁸, this allows single-excitation quadruple-emission measurements, even if both FRET pairs are present at the same intracellular location. To verify this method, we expressed SC-SCAT3 and SapRC2, a Ca^{2+} -indicator based on Sapphire and DsRed⁹, in HeLa cells. Upon apoptosis induction with TNF- α , we observed Ca^{2+} oscillation within the first 90 min, and then it ceased¹⁰; in contrast, we observed caspase-3 activation at around 120 min after induction (**Fig. 3**, **Supplementary Video 2** and **Supplementary Note 2** online). Such dual FRET imaging should allow a variety of experiments to elucidate the dynamic relationships among multiple biological phenomena in a single cell.

Accession codes. GenBank, EMBL Nucleotide Sequence Database and DNA Databank of Japan: AB444952 (nucleotide sequence encoding Sirius).

Note: Supplementary information is available on the Nature Methods website.

ACKNOWLEDGMENTS

We thank R.E. Campbell (University of Alberta) and A. Miyawaki (RIKEN) for providing the cDNA encoding EBFP2 and SapRC2, respectively. This work was partly supported by grants from Scientific Research on Advanced Medical Technology of the Ministry of Labor, Health and Welfare of Japan and the Japanese Ministry of Education, Science and Technology.

AUTHOR CONTRIBUTIONS

W.T. performed experiments and data analysis; T.M. and I.K. contributed to gene construction; T.T., To.N. and K.S. set up microscopy systems; K.H. contributed to imaging of phagocytosis; Ta.N. contributed to the conceptual development, experimental design, data analysis and manuscript preparation.

Published online at <http://www.nature.com/naturemethods/>
Reprints and permissions information is available online at <http://npg.nature.com/reprintsandpermissions/>

- Cubitt, A.B. *et al. Trends Biochem. Sci.* **20**, 448–455 (1995).
- Matsuda, T., Miyawaki, A. & Nagai, T. *Nat. Methods.* **5**, 339–345 (2008).
- Nagai, T. *et al. Nat. Biotechnol.* **20**, 87–90 (2002).
- Ai, H.W., Shaner, N.C., Cheng, Z., Tsieng, R.Y. & Campbell, R.E. *Biochemistry* **46**, 5904–5910 (2007).
- Xu, X. *et al. Nucleic Acids Res.* **26**, 2034–2035 (1998).
- Takemoto, K., Nagai, T., Miyawaki, A. & Miura, M. *Cell Biol.* **160**, 235–243 (2003).
- Ai, H.W., Hazelwood, K.L., Davidson, M.W. & Campbell, R.E. *Nat. Methods.* **5**, 401–403 (2008).
- Zimmermann, T., Rietdorf, J. & Pepperkok, R. *FEBS* **546**, 87–92 (2003).
- Mizuno, H., Sawano, A., Eli, P., Hama, H. & Miyawaki, A. *Biochemistry* **40**, 2502–2510 (2001).
- Pu, Y., Luo, K.Q. & Chang, D.C.A. *Biochem. Biophys. Res. Commun.* **299**, 762–769 (2002).

An ultramarine fluorescent protein with increased photostability and pH insensitivity

Wataru Tomosugi, Tomoki Matsuda, Tomomi Tani, Tomomi Nemoto, Ippei Kotera, Kenta Saito, Kazuki Horikawa & Takeharu Nagai

Supplementary figures and text:

| Supplementary File | Title |
|-------------------------------|--|
| Supplementary Figure 1 | Sequence alignment of UMFP and GFP variants. |
| Supplementary Figure 2 | Comparative characterization of the absorption and fluorescence properties of UMFP variants. |
| Supplementary Figure 3 | Multi color imaging of HeLa cells stained by four color variants of fluorescent protein. |
| Supplementary Figure 4 | Dual color imaging of UMFP-mito and EBFP-H2B in HeLa cells by linear spectral unmixing. |
| Supplementary Figure 5 | Fluorescence emission intensity of Sirius, EBFP, and EBFP2 at 37 °C. |
| Supplementary Figure 6 | HeLa cells expressing Sirius or a Sirius fusion protein. |
| Supplementary Figure 7 | Dual FRET imaging by single-excitation-quadruple-emission measurement mode. |
| Supplementary Table 1 | Förster radius (nm) of the fluorescent protein pairs. |
| Supplementary Note 1 | Photobleaching of CFP. |
| Supplementary Note 2 | Linear unmixing of dual FRET measurement. |
| Supplementary Methods | |

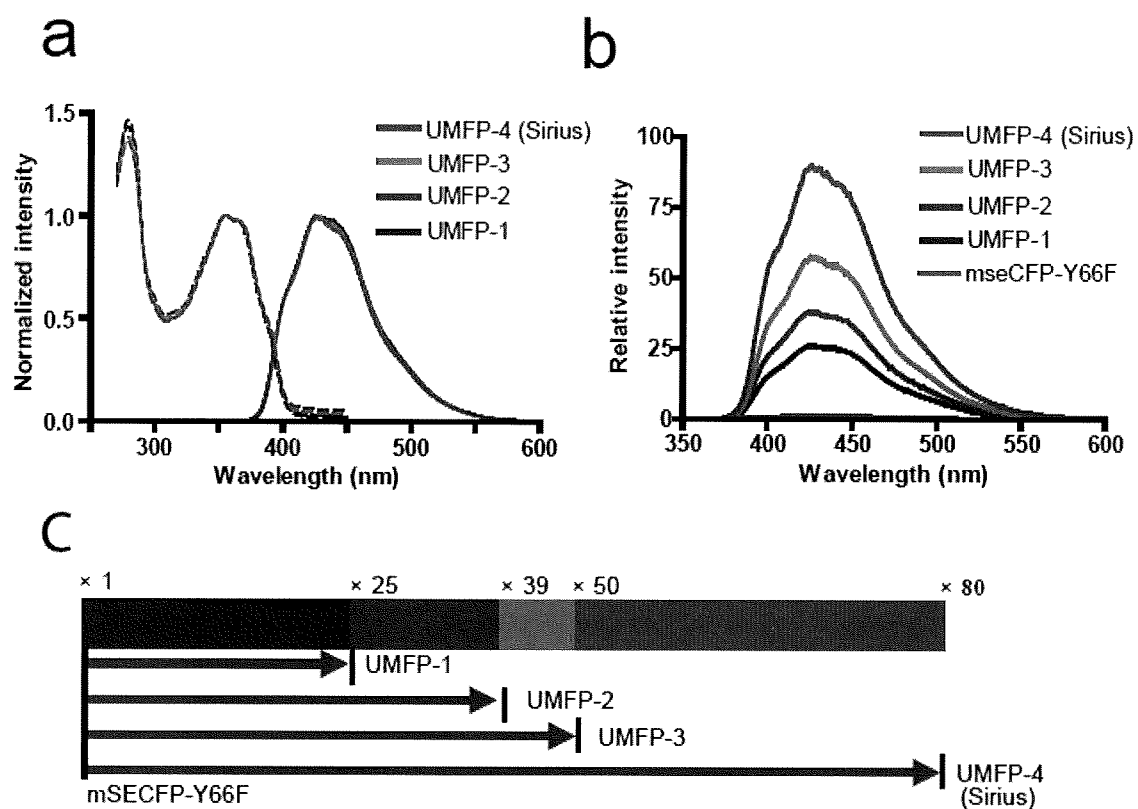
Note: Supplementary Videos 1 and 2 are available on the Nature Methods website.

Supplementary Figure 1. Sequence alignment of UMFP and GFP variants.

| | | | | | | | | | | | | | | | | | | | | | | | | | | | | | |
|-----------------|-----|----------------------------------|-----|----|----|----|----|----|----|----|----|----|----|----|----|----|----|-----|---|---|---|---|---|---|---|---|---|---|-----|
| wtGFP | 1 | MVSKGEELFTGVVPIILVELDGDVNGHKFSVS | GE | EG | DA | TY | GK | LL | KF | IC | TT | GK | LP | VP | WT | 60 | | | | | | | | | | | | | |
| EBFP | 1 | MVSKGEELFTGVVPIILVELDGDVNGHKFSVS | GE | EG | DA | TY | GK | LL | KF | IC | TT | GK | LP | VP | WT | 60 | | | | | | | | | | | | | |
| ECFP | 1 | MVSKGEELFTGVVPIILVELDGDVNGHKFSVS | GE | EG | DA | TY | GK | LL | KF | IC | TT | GK | LP | VP | WT | 60 | | | | | | | | | | | | | |
| mseCFP | 1 | MVSKGEELFTGVVPIILVELDGDVNGHRS | VS | GE | EG | DA | TY | GK | LL | KF | IC | TT | GK | LP | VP | WT | 60 | | | | | | | | | | | | |
| mseCFP-Y66F | 1 | MVSKGEELFTGVVPIILVELDGDVNGHRS | VS | GE | EG | DA | TY | GK | LL | KF | IC | TT | GK | LP | VP | WT | 60 | | | | | | | | | | | | |
| UMFP-1 | 1 | MVSKGEELFTGVVPIILVELDGDVNGHRS | VS | GE | EG | DA | TY | GK | LL | KF | IC | TT | GK | LP | VP | WT | 60 | | | | | | | | | | | | |
| UMFP-2 | 1 | MVSKGEELFTGVVPIILVELDGDVNGHRS | VS | GE | EG | DA | TY | GK | LL | KF | IC | TT | GK | LP | VP | WT | 60 | | | | | | | | | | | | |
| UMFP-3 | 1 | MVSKGEELFTGVVPIILVELDGDVNGHRS | VS | GE | EG | DA | TY | GK | LL | KF | IC | TT | GK | LP | VP | WT | 60 | | | | | | | | | | | | |
| UMFP-4 (Sirius) | 1 | MVSKGEELFTGVVPIILVELDGDVNGHRS | VS | GE | EG | DA | TY | GK | LL | LI | CI | TT | GK | LP | VP | WT | 60 | | | | | | | | | | | | |
| wtGFP | 61 | LVITTFSYGVCFSRYPDHMKQHDFFKSAM | PE | GY | VE | RT | IF | FK | DD | GN | YK | TR | AE | VK | FE | GD | TL | 120 | | | | | | | | | | | |
| EBFP | 61 | LVITTFSHGVCFSRYPDHMKQHDFFKSAM | PE | GY | VE | RT | IF | FK | DD | GN | YK | TR | AE | VK | FE | GD | TL | 120 | | | | | | | | | | | |
| ECFP | 61 | LVITTFITWVCFSRYPDHMKQHDFFKSAM | PE | GY | VE | RT | IF | FK | DD | GN | YK | TR | AE | VK | FE | GD | TL | 120 | | | | | | | | | | | |
| mseCFP | 61 | LVITTFITWVCFFARYPDHMKQHDFFKSAM | PE | GY | VE | RT | IF | FK | DD | GN | YK | TR | AE | VK | FE | GD | TL | 120 | | | | | | | | | | | |
| mseCFP-Y66F | 61 | LVITTFITWVCFFARYPDHMKQHDFFKSAM | PE | GY | VE | RT | IF | FK | DD | GN | YK | TR | AE | VK | FE | GD | TL | 120 | | | | | | | | | | | |
| UMFP-1 | 61 | LVITTFITWVCFFARYPDHMKQHDFFKSAM | PE | GY | VE | RT | IF | FK | DD | GN | YK | TR | AE | VK | FE | GD | TL | 120 | | | | | | | | | | | |
| UMFP-2 | 61 | LVITTFITWVCFFARYPDHMKQHDFFKSAM | PE | GY | VE | RT | IF | FK | DD | GN | YK | TR | AE | VK | FE | GD | TL | 120 | | | | | | | | | | | |
| UMFP-3 | 61 | LVITTFITWVCFFARYPDHMKQHDFFKSAM | PE | GY | VE | RT | IF | FK | DD | GN | YK | TR | AE | VK | FE | GD | TL | 120 | | | | | | | | | | | |
| UMFP-4 (Sirius) | 61 | LVITTFITWVLCFFARYPDHMKQHDFFKSAM | PE | GY | VE | RT | IF | FK | DD | GN | YK | TR | AE | VK | FE | GD | TL | 120 | | | | | | | | | | | |
| wtGFP | 121 | VNRIELKGLDFKEDGNILGHKLEYNNSHN | VYI | MA | D | K | K | N | G | T | K | V | N | F | K | I | R | H | N | I | E | D | G | S | V | Q | L | A | 180 |
| EBFP | 121 | VNRIELKGLDFKEDGNILGHKLEYNNSHN | VYI | MA | D | K | K | N | G | T | K | V | N | F | K | I | R | H | N | I | E | D | G | S | V | Q | L | A | 180 |
| ECFP | 121 | VNRIELKGLDFKEDGNILGHKLEYNNTSH | VYI | MA | D | K | K | N | G | T | K | A | H | E | K | I | R | H | N | I | E | D | G | S | V | Q | L | A | 180 |
| mseCFP | 121 | VNRIELKGLDFKEDGNILGHKLEYNNTSH | VYI | MA | D | K | K | N | G | T | K | A | H | E | K | I | R | H | N | I | E | D | G | S | V | Q | L | A | 180 |
| mseCFP-Y66F | 121 | VNRIELKGLDFKEDGNILGHKLEYNNTSH | VYI | MA | D | K | K | N | G | T | K | A | H | E | K | I | R | H | N | I | E | D | G | S | V | Q | L | A | 180 |
| UMFP-1 | 121 | VNRIELKGLDFKEDGNILGHKLEYNNTSH | VYI | MA | D | K | K | N | G | T | K | A | H | E | K | I | R | H | N | I | E | D | G | S | V | Q | L | A | 180 |
| UMFP-2 | 121 | VNRIELKGLDFKEDGNILGHKLEYNNTSH | VYI | MA | D | K | K | N | G | T | K | A | H | E | K | I | R | H | N | I | E | D | G | S | V | Q | L | A | 180 |
| UMFP-3 | 121 | VNRIELKGLDFKEDGNILGHKLEYNNTSH | VYI | MA | D | K | K | N | G | T | K | A | H | E | K | I | R | H | N | I | E | D | G | S | V | Q | L | A | 180 |
| UMFP-4 (Sirius) | 121 | VNRIELKGLDFKEDGNILGHKLEYNNTSH | VYI | MA | D | K | K | N | G | T | K | A | H | E | K | I | R | H | N | I | E | D | G | S | V | Q | L | A | 180 |
| wtGFP | 181 | DHYQONTPIGDGPVLLPDNNHYLSQSALS | KD | PN | E | K | R | D | H | M | V | L | E | F | V | T | A | A | C | I | L | G | M | D | E | L | Y | K | 239 |
| EBFP | 181 | DHYQONTPIGDGPVLLPDNNHYLSQSALS | KD | PN | E | K | R | D | H | M | V | L | E | F | V | T | A | A | C | I | L | G | M | D | E | L | Y | K | 239 |
| ECFP | 181 | DHYQONTPIGDGPVLLPDNNHYLSQSALS | KD | PN | E | K | R | D | H | M | V | L | E | F | V | T | A | A | C | I | L | G | M | D | E | L | Y | K | 239 |
| mseCFP | 181 | DHYQONTPIGDGPVLLPDNNHYLSQSALS | KD | PN | E | K | R | D | H | M | V | L | E | F | V | T | A | A | C | I | L | G | M | D | E | L | Y | K | 239 |
| mseCFP-Y66F | 181 | DHYQONTPIGDGPVLLPDNNHYLSQSALS | KD | PN | E | K | R | D | H | M | V | L | E | F | V | T | A | A | C | I | L | G | M | D | E | L | Y | K | 239 |
| UMFP-1 | 181 | DHYQONTPIGDGPVLLPDNNHYLSQSALS | KD | PN | E | K | R | D | H | M | V | L | E | F | V | T | A | A | C | I | L | G | M | D | E | L | Y | K | 239 |
| UMFP-2 | 181 | DHYQONTPIGDGPVLLPDNNHYLSQSALS | KD | PN | E | K | R | D | H | M | V | L | E | F | V | T | A | A | C | I | L | G | M | D | E | L | Y | K | 239 |
| UMFP-3 | 181 | DHYQONTPIGDGPVLLPDNNHYLSQSALS | KD | PN | E | K | R | D | H | M | V | L | E | F | V | T | A | A | C | I | L | G | M | D | E | L | Y | K | 239 |
| UMFP-4 (Sirius) | 181 | DHYQONTPIGDGPVLLPDNNHYLSQSALS | KD | PN | E | K | R | D | H | M | V | L | E | F | V | T | A | A | C | I | L | G | M | D | E | L | Y | K | 239 |

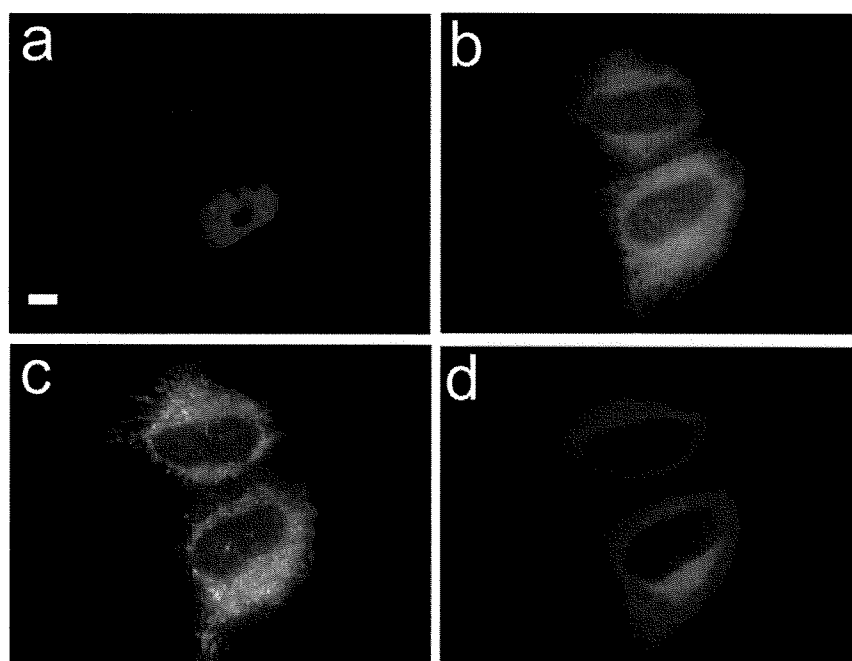
Sequences show the alignment of *Aequorea victoria* wild-type GFP, EBFP, ECFP, mseCFP, mseCFP-Y66F, UMFP-1, UMFP-2, UMFP-3 and UMFP-4(Sirius). The texts on gray background show the retained amino acids for mutagenesis. Mutations related to UMFP-4(Sirius) are indicated as white text on a black background.

Supplementary Figure 2. Comparative characterization of the absorption and fluorescence properties of UMFP variants.



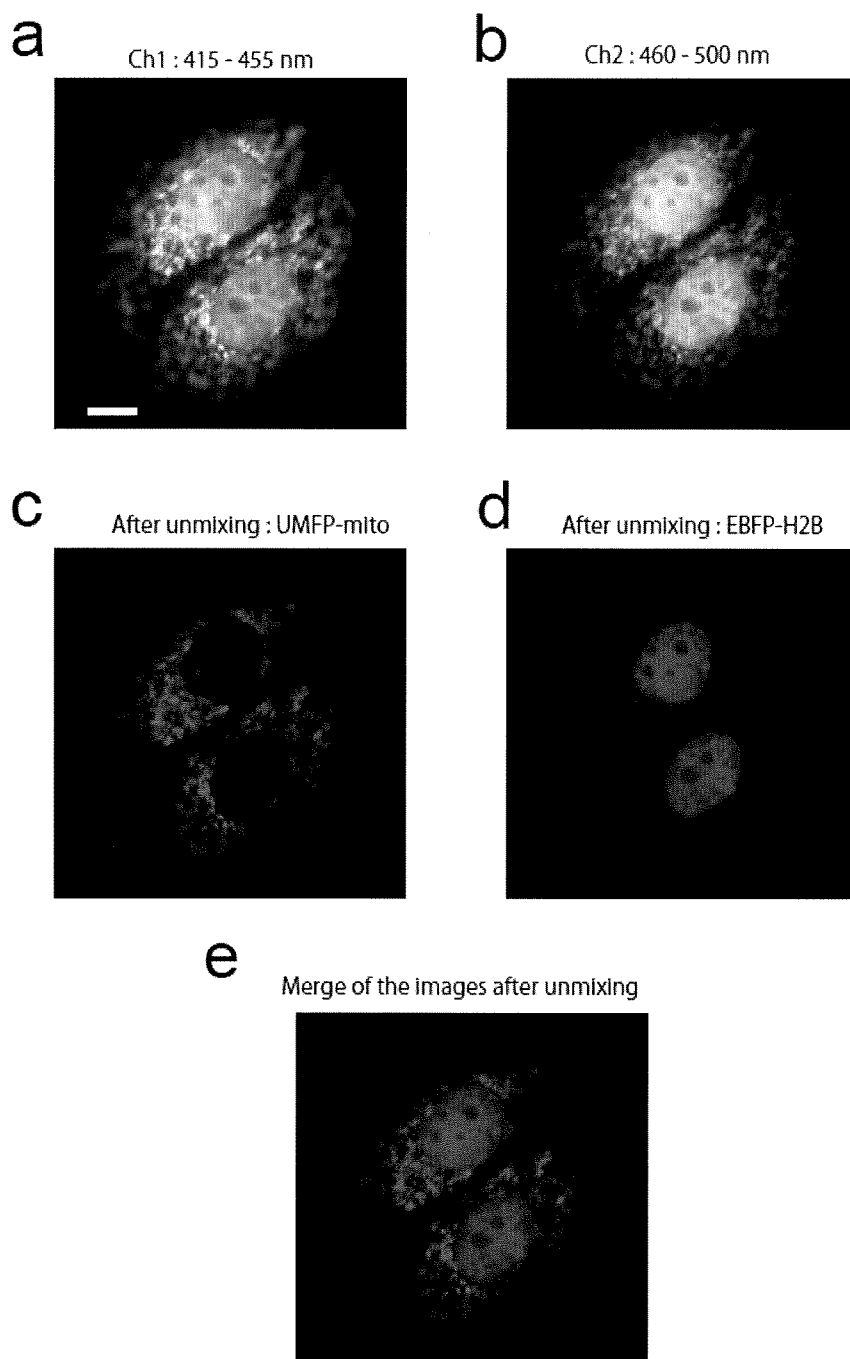
(a) Absorption (dotted lines) and emission spectra (solid lines) of UMFP variants. **(b)** Fluorescence emission spectra of purified UMFP variants: msecCFP-Y66F, UMFP-1, UMFP-2, UMFP-3, and UMFP-4. **(c)** Brightness of fluorescence by calculation of extinction coefficient and quantum yield of UMFP variants. Brightness was normalized to the fluorescence of msecCFP-W66F.

Supplementary Figure 3. Multi color imaging of HeLa cells stained by four color variants of fluorescent protein.



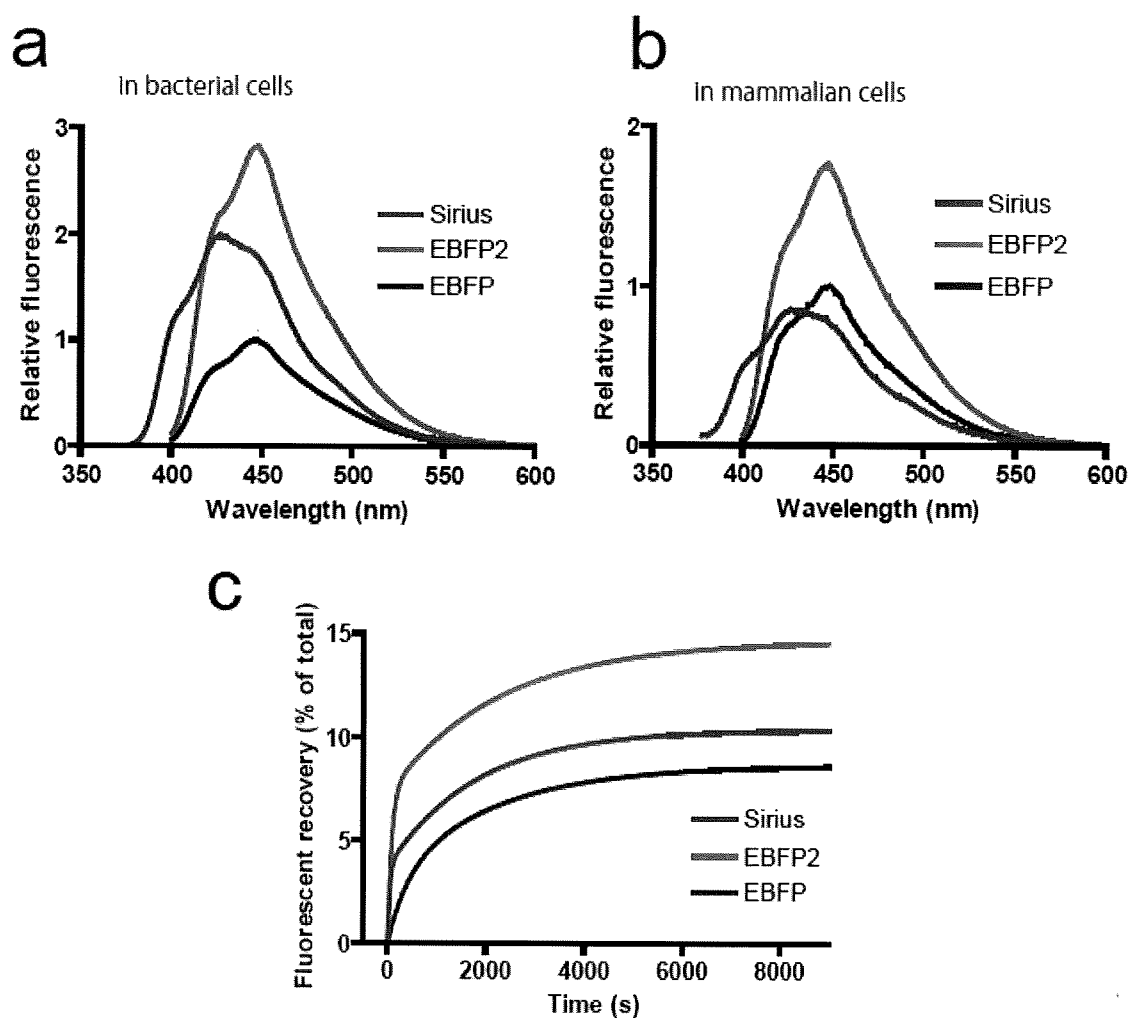
(a) UMFP-1-labeled nuclei, (b) mseCFP-labeled endoplasmic reticulum, (c) Venus-labeled mitochondria, (d) mCherry-labeled microtubules, Scale bar, 10 μm

Supplementary Figure 4. Dual color imaging of UMFP-mito and EBFP-H2B in HeLa cells by linear spectral unmixing.



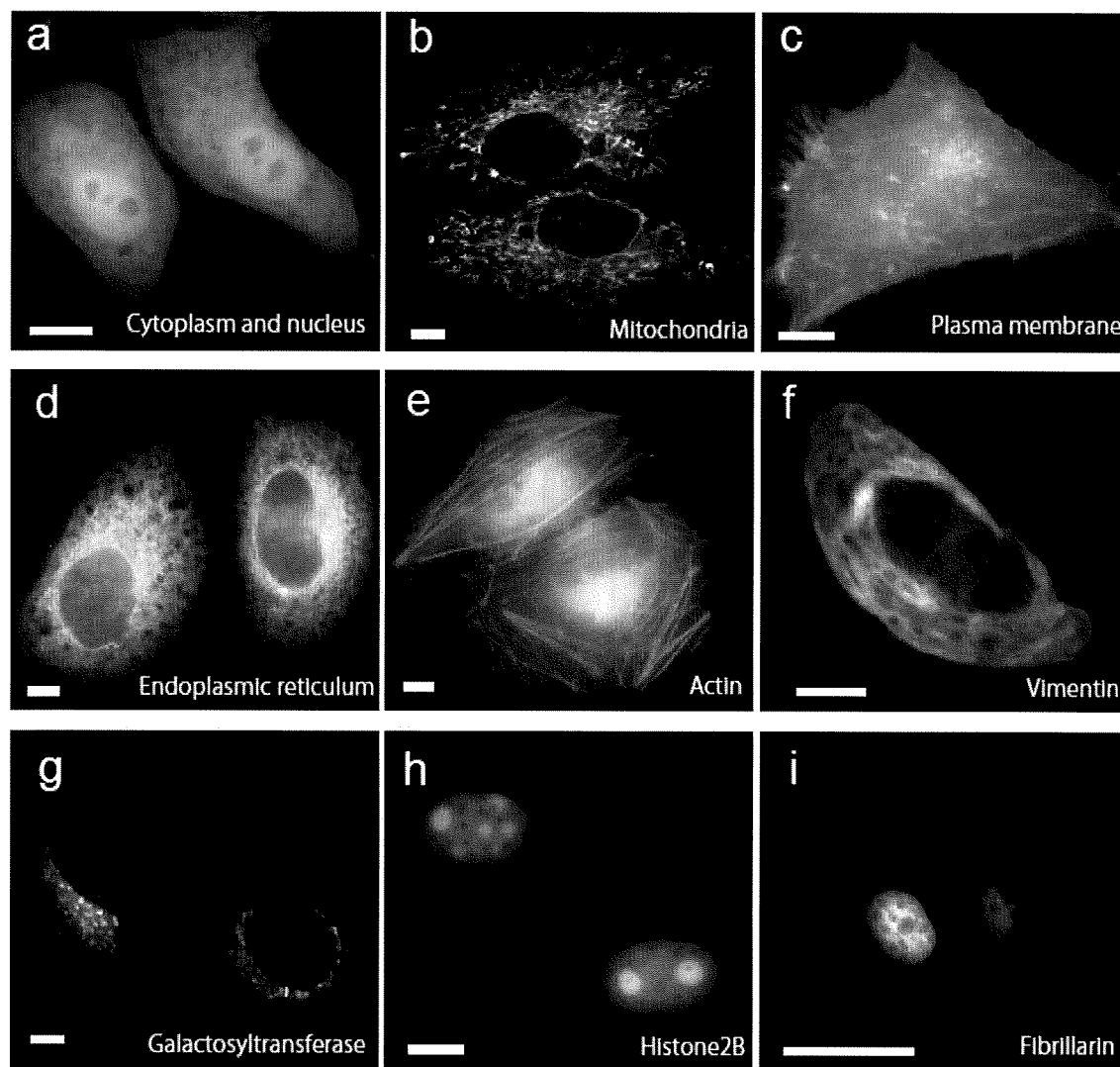
(a, b) Fluorescence images taken through detection channel 1 (Ch1: 415 - 455 nm) (a) and detection channel 2 (Ch2: 459 - 499 nm) (b). **(c, d)** Fluorescence images of UMFP-mito (c: green) and EBFP-H2B (d: magenta) after linear spectral unmixing. **(e)** The image created by merging the images in c and d. Scale bar, 10 μ m.

Supplementary Figure 5. Fluorescence emission intensity of Sirius, EBFP, and EBFP2 at 37 °C.



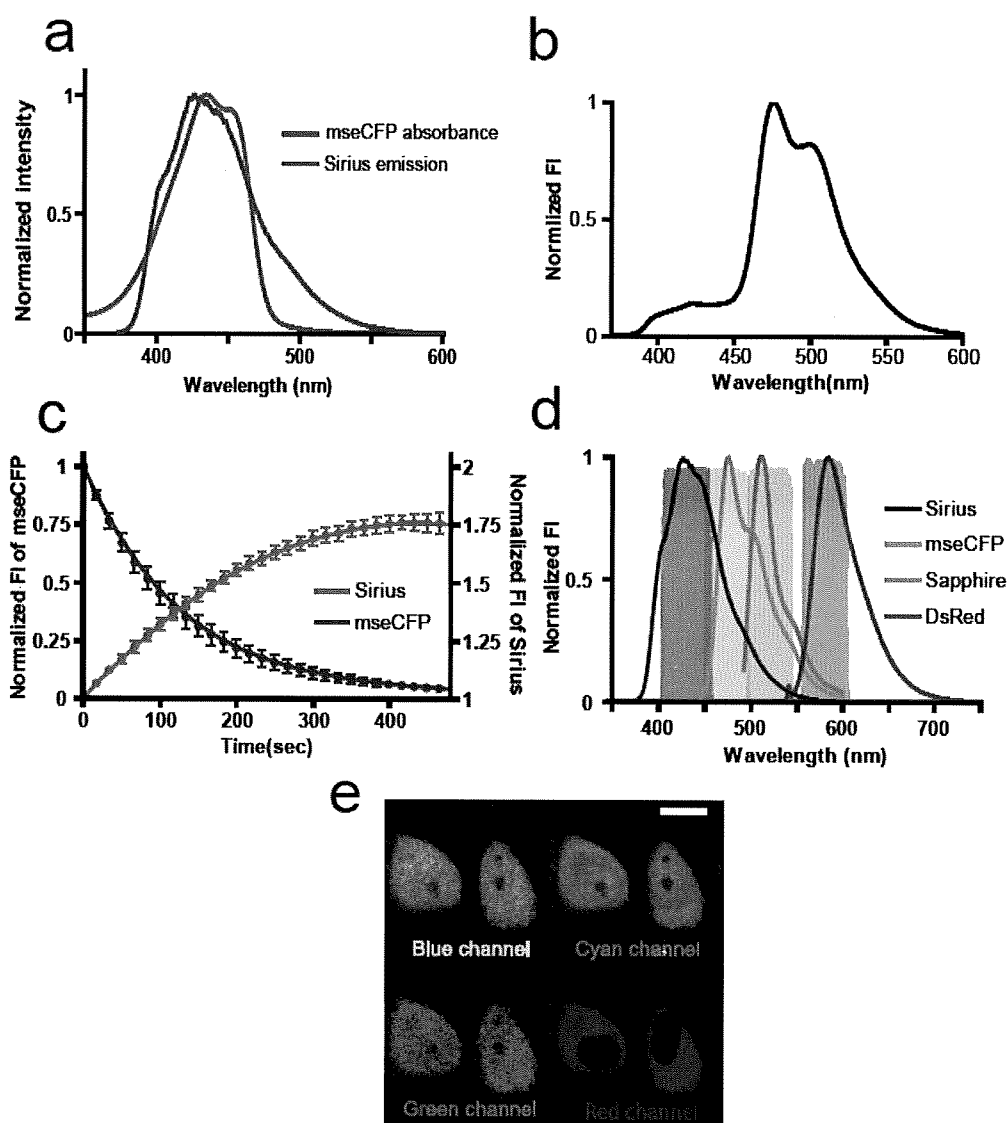
Relative emission spectra in *E. coli* (a) and HEK293 cells (b) cultured at 37 °C. Sirius was excited at 355 nm. EBFP2 and EBFP were excited at 380 nm. (c) Fluorescence acquisition curve of Sirius (red), EBFP2 (cyan), and EBFP (blue) in solution at 37 °C.

Supplementary Figure 6. HeLa cells expressing Sirius or a Sirius fusion protein.



(a) Sirius, **(b)** Sirius-mito, **(c)** Sirius-pm, **(d)** Sirius-er, **(e)** Sirius-actin, **(f)** Sirius-vimentin, **(g)** Sirius-Golgi, **(h)** Sirius-H2B, and **(i)** Sirius-fibrillarin Scale bars, 10 μ m.

Supplementary Figure 7. Dual FRET imaging by single-excitation-quadruple-emission measurement mode.



(a) Spectral overlap between Sirius emission (red) and mseCFP absorption (cyan). (b) The emission spectrum of purified Sirius-mseCFP fusion protein by excitation at 360 nm. (c) Time course of changing in fluorescence intensity of Sirius and mseCFP in Sirius-mseCFP fusion protein during acceptor photobleaching. Error bars are s.d (n=3). (d) The emission spectrum of Sirius, mseCFP, Sapphire, and DsRed. Transparent colors represent the emission filters used to acquire each fluorescent protein signal for the dual FRET imaging. (e) Dual-FRET imaging of SC-SCAT3 and SapRC2 in HeLa cells by two-photon excitation at 720nm. Scale bars, 30 μ m.

Supplementary Table 1. Förster radius (nm) of the fluorescent protein pairs.

| | | Donor | | | | | |
|-----------------|--------|--------------|------|------|------|------|--------|
| Acceptor | | Sirius | EBFP | ECFP | EGFP | EYFP | DsRed1 |
| | Sirius | — | — | — | — | — | — |
| | EBFP | 2.8 | — | — | — | — | — |
| | ECFP | 3.7 | 3.9 | — | — | — | — |
| | EGFP | 4.0 | 4.2 | 5.2 | — | — | — |
| | EYFP | 3.7 | 3.9 | 4.7 | 5.6 | — | — |
| | DsRed1 | 4.1 | 4.3 | 5.2 | 5.9 | 6.1 | — |

Supplementary Note 1

Photobleaching of CFP. We obtained FRET efficiency in Sirius-mseCFP FRET pair by measuring dequenching of donor (Sirius) emission after acceptor (mseCFP) photobleaching. In the experiment, the fluorescence intensity of Sirius was increased 1.75 fold (**Supplementary Fig. 6c**), from which we calculated about 43% FRET efficiency. However, the increase in Sirius fluorescence might contain the signal from photoconverted mseCFP upon photobleaching. To exclude the possibility of mseCFP photoconversion to a more blue-shifted spectrum especially overlapping with emission spectrum of Sirius, we performed a control experiment to show no photoconversion of mseCFP upon photobleaching. As shown in **Fig. A**, we did not see any detectable photoconversion of mseCFP. Therefore, we concluded that the 43% FRET efficiency in Sirius-mseCFP obtained from the acceptor mseCFP bleaching experiment was appropriate.

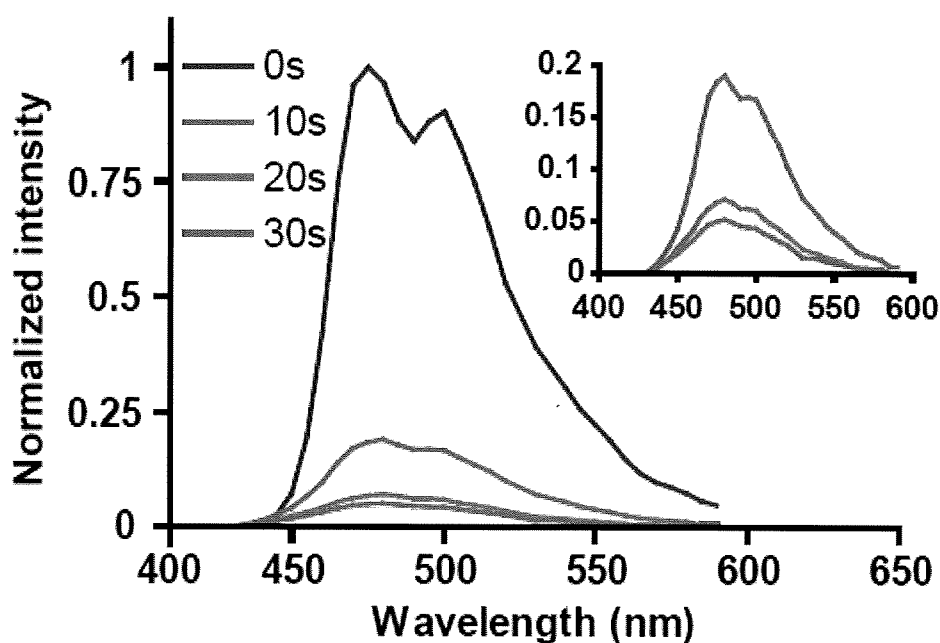
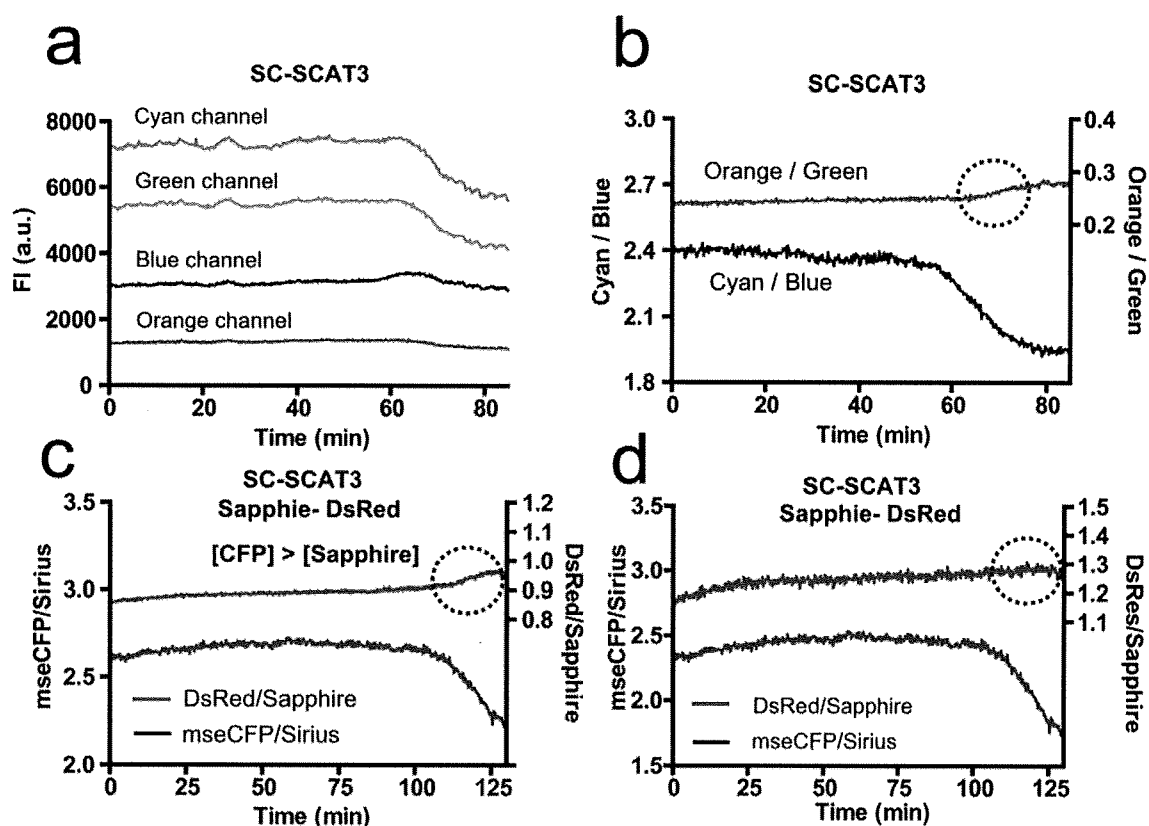


Figure A. Emission spectra of mseCFP during photobleaching in a HeLa cell. mseCFP expressing in living HeLa cells were photobleached by intense excitation with 405 nm laser diode under an inverted microscope. Times indicated in the panel show the total time of photobleaching. An inset graph shows the data with expanded ordinate.

Supplementary Note 2

Linear unmixing of dual FRET measurement. Although the two FRET pairs, Sirius-mseCFP and Sapphire-DsRed have an advantage such that they can use common excitation wavelength since both Sirius and Sapphire can be excited at 380 nm. However, we have to carefully consider bleed through signals of Sirius and mseCFP into channels for Sapphire and DsRed detection (**Fig. Ba**) because the bleed through signals greatly influence to DsRed/Sapphire emission ratio value (**Fig. Bb**), especially when mseCFP intensity signal is much larger than that of Sapphire (**Fig. Bc**). In this case, spectral unmixing technique can be used to remove the bleed through signal (**Fig. Bd**). We also confirmed this by co-expressed SC-SCAT3 and SapRC2 in HeLa cells (compare **Fig. Be**, **Fig. Bf** and **Fig. 3c**) Meanwhile, we might be able to minimize the bleed through effect by choosing cells with larger Sapphire signal than that of mseCFP because the relatively small mseCFP signal does not significantly influence the value of DsRed/Sapphire emission ratio (**Fig. Bg,h**).



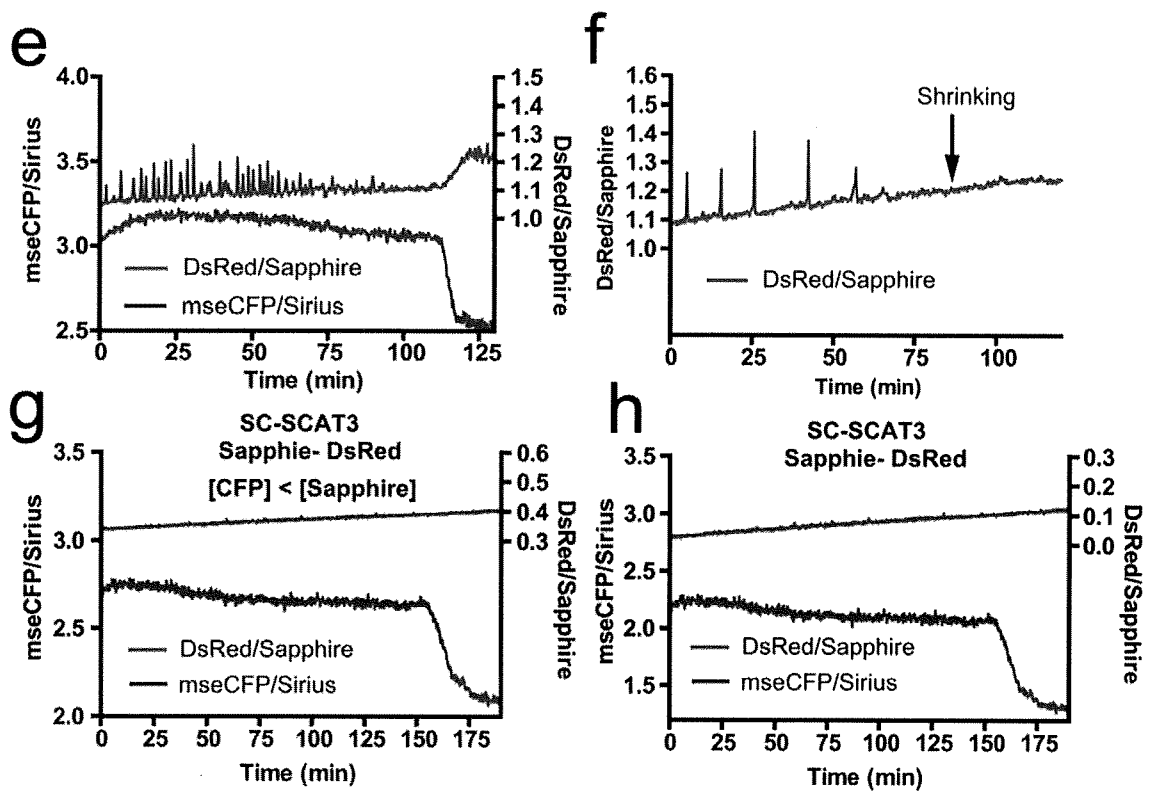


Figure B. The effect of bleed through on intensity ratio. (a,b) Time course of the fluorescence intensity (a) and intensity ratio (b) of HeLa cells expressing only SC-SCAT3 measuring through the emission filters for blue, cyan, green and orange acquisition. a.u, arbitrary units. Dotted circles indicate the change of ratio derived from bleed through. (c, d) Time course of intensity ratio in HeLa cells expressing both SC-SCAT3 and Sapphire-DsRed (joined by a LE amino acid) without (c) and with (d) four colors unmixing. Shown is the result obtained from the cells in which fluorescence intensity of mseCFP is larger than that of Sapphire. (e) Time course of the intensity ratio of both mseCFP/Sirius (blue line) and DsRed/Sapphire (red line) before four colors unmixing in the regions of interest shown in Fig.3a. (f) Time course of the intensity ratio of HeLa cells expressing only SapRC2 measuring after TNF-alpha treatment. The arrow indicates the start of cell shrinking. (g, h) Time course of intensity ratio in HeLa cells expressing both SC-SCAT3 and Sapphire-DsRed (joined by a LE amino acid) without (g) and with (h) four colors unmixing. Shown is the result obtained from the cells in which fluorescence intensity of mseCFP is smaller (g, h) than that of Sapphire.

Supplementary Methods

Gene construction. The Sirius-mseCFP fusion protein was made by coupling C-terminally truncated Sirius and N-terminally truncated mseCFP, as shown previously¹². The cDNA of C-terminally truncated Sirius was amplified by PCR using a sense primer, 5'-GCGGATCCGATGGTGAGCAAGGGCGAGGAG-3', containing a *Bam*HI site, and an antisense primer, 5'-TTATCTCGAGGGCGGCGGTACGAACTCCA-3', containing an *Xho*I site before the Ala227 codon of Sirius. The cDNA of N-terminally truncated mseCFP was amplified by PCR using a sense primer, 5'-GCCTCGAGGAGGAGCTGTTCACCGGG-3', containing an *Xho*I site before the codon for Glu5 and an antisense primer, 5'-GCGAATTCTTACTTGTACAGCTCGTCCATGC-3', containing a termination codon followed by an *Eco*RI site. The restriction products were cloned into the *Bam*HI and *Eco*RI sites of pRSET_B (Invitrogen) for bacterial expression. For mammalian expression, the *Bam*HI-*Eco*RI fragment of Sirius-mseCFP was subcloned into pcDNA3 (Invitrogen). UMFP1-H2B and EBFP-H2B in mammalian expression vectors were constructed by replacing the Phamret in Phamret-H2B-pcDNA3² with UMFP-1 and EBFP, respectively. mCherry-Tub and Venus-mito in mammalian expression vectors were constructed by replacing EYFP in pEYFP-Tub (Clontech) with mCherry¹³, and by fusing the 12 N-terminal amino acids of the cytochrome c oxidase subunit IV presequence to the N terminus of Venus³, respectively. mseCFP-er was generated by extending mseCFP at the N terminus with the signal peptide from calreticulin and at the C terminus with an ER retention signal¹⁴. For the imaging of Sirius fusion constructs,

Sirius-Mito, Sirius-Golgi, Sirius-H2B, Sirius-fibrillarin and Sirius-Tub in mammalian expression vectors were constructed by replacing the Phamret in Phamret-mit-pcDNA3², Phamret-peroxisome-pcDNA3², Phamret-Golgi-pcDNA3², Phamret-H2B-pcDNA3², Phamret-fibrillarin-pcDNA3², and the EYFP in pEYFP-Tub (Clontech) with Sirius. Sirius-pm was constructed by adding the myristoylation and palmitoylation sequence from lyn kinase (MGCIKSKRKDNLNDDGVDMKT) to N terminus¹⁵. Sirius-er was constructed such as making of mseCFP-er. β -actin and Vimentin were inserted into C-terminal and N-terminal of Sirius in pcDNA3 respectively. β -actin and vimentin have 20 (GGSGGSGGSGGSGGQFQIST) amino acid residues and 18 (GDPPVATGGSGGSGGSGG) amino acid residues as linker peptide. UC-SCAT3-pcDNA3.1(-) was constructed by replacing Venus in SCAT3-pcDNA3.1(-)⁵ with Sirius. The SapRC2-pcDNA3⁸ was kindly provided by Dr. Atsushi Miyawaki. The cDNA sequences for all the fluorescent protein variants were confirmed by dye terminator cycle sequencing using Big Dye (Applied Biosystems).

Screening. After transformation of *Escherichia coli* [JM109(DE3)] with the mutagenized DNAs, the bacteria were grown up on agar plates (10 cm in diameter) at 37°C for 16 hrs to allow the fluorescence to develop. Colonies with brighter fluorescence were picked under a MVX10 Macro View microscope with a U-MWU2 filter cube (BP330-385 excitation filter, DM400 dichroic mirror, and BA420 emission filter), and cultured overnight in 1.5 mL of LB medium containing 0.1 mg/mL carbenicillin.

Spectroscopy. Absorption spectra of the purified fluorescent proteins were measured on

a V-630 BIO spectrophotometer (Jasco). The protein concentrations used to calculate molar extinction coefficients were determined by the Bradford method (Protein assay kit, Bio-Rad). The fluorescent excitation and emission spectra were measured on an F-2500 fluorescence spectrophotometer (Hitachi). Fluorescence quantum yields were measured using a Hamamatsu Photonics C9920-01, an absolute photoluminescence quantum-yield measurement device.

Measurement of fluorescence intensity at 37 °C. *E. Coli* were transformed with Sirius-pRSET_B, EBFP2-pRSET_B and EBFP-pRSET_B. After 16h culture on the LB plate at 37 °C, colonies were picked up and transfer into 2ml LB solution. After 12h culture in LB solution at 37°C, cultures were centrifuged and the pellet were suspended by PBS buffer. The bacteria suspension were diluted to OD₆₀₀ = 0.2 . The diluted solution was used for measuring the emission spectra. Measurements were done on three independent colonies. Transfection and culture of HEK293 cells were performed by FreeStyle™ 293 Expression System (invitrogen). Namely, approximately 30 µg Sirius-pcDNA3, EBFP2-pcDNA3 and EBFP-pcDNA3 were transfected into FreeStyle™ 293-F cells with concentration of 1 x 10⁶ cells/ml. After 24h culture in the medium at 37 °C, cultures were centrifuged and the pellet were suspended by PBS buffer sufficiently. The cells suspension was used in order to measure the emission spectra. For standardization of fluorescent protein amount, western blotting was carried out. Anti-GFP Polyclonal Antibody (MBL) and anti-rabbit IgG HRP (Promega) were used for primary and secondary antibody respectively. In order to detect the chemi-luminescence of HRP, SurperSignal West Dura Extended Duration Substrate Antibodies (PIERCE) was used. Purified EGFP was used as a standard of the intensity of the band. The independent

transfection was done two times.

Measurement of protein maturation kinetics. The oxidation kinetics of the chromophore was assessed as described¹⁶. Briefly, fluorescent proteins were denatured and rehydrated by incubation for 5 min at 95 °C in buffer containing 8 M urea, 1 mM DTT, and 5 mM sodium dithionite. Renaturation was initiated by 100-fold dilution in buffer containing 50 mM Tris-HCl pH 7.5, 35 mM KCl, 2 mM MgCl₂, 1 mM DTT at 37 °C. An equal amount of native protein was used for the normalization of fluorescence recovery.

pH titration. Fluorescent proteins were diluted to 2 μM in a series of 50 mM titration buffers. Glycine-HCl (pH 3.0 and 3.4), NaOAc (pH 3.8 and 5.4), MES (pH 5.8 and 6.2), MOPS (pH 6.6 and 7.0), HEPES (pH 7.4 and 7.8), and Glycine (pH 8.6 and 9.0) were used as the pH buffers. The pK_a was determined by fitting the data to the sigmoidal dose-response equation.

Measurement of photostability. Fluorescent proteins expressed in HeLa cells were photobleached using a mercury arc-lamp–equipped TE2000E inverted microscope (Nikon) with an Apo-VC 40x, 1.30 NA oil-immersion objective (Nikon), and FF01-370/36, CFW-Di01-Clin, and FF01-435/40 (all from Semrock) as the excitation filter, dichroic mirror, and emission filter, respectively. Neutral density filters were removed, and fluorescence images of HeLa cells were taken every 10 sec with a 10-ms exposure time using a cooled CCD camera, ORCA-AG (Hamamatsu Photonics) under the control software, AquaCosmos (Hamamatsu Photonics). Laser photobleaching was

performed with a 375-nm laser, CUBE 375-16c (Coherent) and using the identical objective, dichroic mirror, and emission filter as in the arc-lamp assays. The bleaching curve was obtained by fitting the time course of the fluorescence intensity data to a single exponential decay. In case of the Sirius, τ_{bleach} which represent the time necessary to bleach 1/e of initial fluorescent intensity, was calculated from data after reaching exponential decay state. The quantum yield for photobleaching was calculated from the decay curve of mercury arc-lamp using the extinction coefficient and τ_{bleach} as described previously¹⁷. The extinction coefficient for this calculation was measured at 370nm, where is the center wavelength of excitation band pass filter used for bleach imaging.

Measurement of fluorescence intensity with two-photon excitation microscopy. The fluorescent proteins expressed in HeLa cells were excited by a mode-locked Ti:Sapphire laser, Tsunami (Spectra physics) at 780nm. The fluorescence of Sirius, EBFP2 and EBFP were detected through interference filter FF01-435/40. Relative fluorescence intensity was obtained using 30 HeLa cells which selected randomly from 3 independent dishes (10 HeLa cells were chosen from 1 dish). Measurements were done after 24h from transfections.

Measurement of FRET efficiency. Sirius-mseCFP fusion protein expressing in HeLa cells was subjected to acceptor photobleaching¹⁸. The FRET efficiency (Et) of the donor-acceptor pair was calculated according to the following equation,

$$Et = 1 - F_{DA} / F_D$$

where F_{DA} and F_D express the fluorescence intensity of the donor (Sirius) before and after acceptor (mseCFP) photobleaching, respectively. For specific photobleaching of

mseCFP, we used EX436/20, DM455 and BA480/40 (all from Nikon) as the excitation filter, dichroic mirror, and emission filter, respectively. Fluorescence intensity of Sirius was measured using FF01-370/36, CFW-Di01-Clin and FF01-435/40 (all from Semrock) as the excitation filter, dichroic mirror, and emission filter, respectively. To exclude a possibility that increase in fluorescence intensity in Sirius channel was due to photoconversion of mseCFP to a more blue-shifted species upon photobleaching, we also performed a control experiment by using HeLa cells expressing only mseCFP, and confirmed no photoconversion (Supplementary Note 1).

Dual FRET and Quadruple-color imaging. Wide-field observation of dual FRET and quadruple color (Sirius, mseCFP, Venus, and mCherry) was performed using the microscopy system described above in the section on *Measurement of photostability*, by alternating the filter blocks for each fluorophore. For dual FRET imaging of SC-SCAT3 and SapRC2, we used a FF01-370/36 excitation filter, a CFW-Di01-Clin dichroic mirror, and emission filters FF01-435/40 for Sirius, FF01-479/40 for mseCFP, FF01-525/39 for Sapphire, and FF01-585/40 for DsRed, all of which were obtained from Semrock. For quadruple color imaging of Sirius, mseCFP, Venus and DsRed, the excitation filters, dichroic mirrors, and emission filters that we used were EX340-380, DM400, and BP435-485 for Sirius, EX436/20, DM455, and BA480/40 for mseCFP, EX500/20, DM515, and BA535/30 for Venus, and 580AF20, 600DRLP, and 630DF30 for mCherry, respectively. The interference filters and dichroic mirrors were obtained from Nikon or Omega Optical. During imaging, the cells were plated in a heated chamber, INUG2-ONI (Tokai Hit) at 37°C.

Linear unmixing of fluorescence spectrum. Linear unmixing of UMFP and EBFP in HeLa cells was carried out by the function of “Multiband Imaging” in AquaCosmos software (Hamamatsu Photonics). We used a FF01-370/36 excitation filter, a CFW-Di01-Clin dichroic mirror, and a FF01-435/40 and FF01-479/40 (all from semrock) for UMFP and EBFP detection, respectively. Linear unmixing of four fluorescence spectra was performed as essentially described previously⁷. Basically, following formula was solved by using the function of “MINVERS” equipped in Microsoft Office Excel 2003.

$$\begin{pmatrix} 1 & Cf_1 & Sa_1 & Ds_1 \\ Si_2 & 1 & Sa_2 & Ds_2 \\ Si_3 & Cf_3 & 1 & Ds_3 \\ Si_4 & Cf_4 & Sa_4 & 1 \end{pmatrix} \begin{pmatrix} I_{Si} \\ I_{Cf} \\ I_{Sa} \\ I_{Ds} \end{pmatrix} = \begin{pmatrix} CH_1 \\ CH_2 \\ CH_3 \\ CH_4 \end{pmatrix}$$

In this formula, CH₁, CH₂, CH₃ and CH₄ indicate total fluorescence intensity in detection channel through emission filters, FF01-435/40, FF01-479/40, FF01-525/39 and FF01-585/40 (Semrock). The normalized spectral contributions of Sirius, CFP, Sapphire, and DsRed to each channel derived from the reference λ -stack data are expressed Si_n, Cf_n, Sa_n, and Ds_n, where subscript n shows the number of channel. The unknown net intensity of Sirius in CH₁, mseCFP in CH₂, Sapphire in CH₃ and DsRed in CH₄ are expressed as I_{Si}, I_{Cf}, I_{Sa} and I_{Ds} respectively.